

Communications

A Versatile PC-Based Range Finding System

P. Saint-Marc, J.-L. Jezouin, and G. Medioni

Abstract—We present an active triangulation-based range finding system composed of an independent laser system generating a sheet of light projected on the object to be measured, which is placed upon a linear or a rotary table driven by a personal computer. This computer includes a video digitizer board to which two cameras, looking at the scene from both sides of the sheet of light, are connected. Besides its low cost, this system has several advantages over similar existing systems. First of all, we use two cameras to limit the well-known occlusion problem and we propose a method to integrate range data obtained from these cameras into a single range image. The calibration of each camera is very simple, provides subpixel accuracy, and is performed only once as the laser or the camera do not move. Our data acquisition uses an interpolation technique that authorizes very accurate depth measurements and our system also provides intensity data in registration with the range data. The application of all these techniques is illustrated by showing numerous examples of the range and intensity data acquisition from various complex objects.

I. INTRODUCTION

There is a strong need in a computer vision research laboratory to have a tool that quickly and efficiently acquires range data. This tool must be integrated in the environment of the laboratory and should be able to bring a piece of a solution to several current research problems, either by providing data for experiments, or by giving a ground truth for some algorithms. We have designed and implemented such a device. Its advantages over existing systems are a very low cost, a simple and fast calibration procedure, and at least comparable performance.

The different range finding techniques can be categorized into three major families: the contrived lighting ranging methods (striped lighting, grid coding, or flying spot), the passive monocular techniques (occlusions clues, texture gradient, focusing, surface orientation) and the passive binocular techniques (stereo disparity). An overview of these different technologies can be found in [1]–[3], [6], [9]. It is important to notice that the methods belonging to the second and third family are still not very well understood and have not yet been implemented to produce operational devices. Furthermore, the development of these techniques requires the availability of precise measurements for the evaluation of their performance.

Out of the existing active ranging techniques (first family), a well-known method consists of projecting a sheet of light on the object to measure by spreading a laser beam light. A video camera (displaced from the light source) is used to record in the image plane the intersection of the sheet of light with the surface of the object. Then, for each point extracted, the corresponding depth is computed by simple triangulation. A complete depth map of the object is obtained by moving the sheet of light [4], [12], or by moving the object itself [8], [11]. Generally, the calibration of such a system

Manuscript received December 19, 1988; revised August 8, 1989. This work was supported by the Defense Advanced Research Projects Agency under Contracts DACA76-85-C-0009 and F33615-87-C-1436, monitored by the U.S. Army Topographic Laboratories and by Wright-Patterson Air Force Base, respectively.

P. Saint-Marc and J.-L. Jezouin were with the Institute for Robotics and Intelligent Systems, University of Southern California, Los Angeles, CA 90089-0273. They are now with Matra MS2I, Signal and Image Processing Laboratory, 78052 Saint-Quentin-en-Yvelines Cedex, France.

G. Medioni is with the Institute for Robotics and Intelligent Systems, University of Southern California, Los Angeles, CA 90089-0273.

IEEE Log Number 9042432.

requires a precise knowledge of the camera parameters, position and orientation with respect to the sheet of light and thus leads to a long and tedious calibration procedure. Another drawback is that, as accurate measurements can only be made with a large displacement of the camera from the light source, large areas of the object surface visible from the light source (illuminated) are not seen from the camera and therefore cannot be measured.

We propose a system that uses a fixed sheet of projected light, a linear (or rotary) table and two cameras. This system differs from previous ones in several ways. First of all, our system is completely PC based and built from commercially available components, which is by itself of major interest. Since the use of a single camera may lead to occlusions, we decided to limit the problem by adding a second camera placed on the other side of the sheet of light. The depth measurements are made independently from each camera. We propose a method that later integrates the range data obtained from both cameras. Another difference is that our calibration procedure does not require any knowledge of the parameters of the cameras and/or the geometry of the system. This calibration is performed only once, using a calibration gauge that permits direct estimation of the geometric transformation from the image plane of each camera to the laser plane (sheet of light). Each geometric transformation is then used to obtain the corresponding positions in the laser plane of the points extracted in the image plane of each camera. These points are extracted using an interpolation technique that provides very accurate depth measurements. Our system also delivers intensity data (in the frequency band of the laser light) in registration with these range data.

In Section II, after a general description of our range finding system, we present our camera calibration procedure and our range and intensity data acquisition. Then in Section III, the integration of the range data obtained for both cameras is shown. In Section IV, we present results of depth and intensity measurements obtained from several complex objects and discuss the quality of the results. Finally, we provide in Section V some concluding remarks.

II. DESCRIPTION OF THE SYSTEM

A schematic diagram of the general configuration of the system is shown in Fig. 1. The object to measure is placed on a high-accuracy New England Affiliated Technologies linear [Fig. 1(a)] or rotary [Fig. 1(b)] table driven through a controller by an IBM PC-AT personal computer. The smallest step size is $1/200^\circ$ for the rotary table and $1/1000$ in for the linear table. An independent laser system generates a plane of light by spreading a laser beam using a vibrating mirror. This plane of light intersects the surface of the object along a 2-D curve. Two Sony XC-38 CCD cameras (280×485 TV line resolution camera with a 16-mm focal length lens) connected to a Matrox PIP-512 video digitizer board ($512 \times 512 \times 8$ bits) plugged into the personal computer are looking toward the illuminated object from both sides of the laser plane. For each camera, the projection of the 2-D curve in the image plane is extracted. If we accurately know the geometric transformation that back-projects any point of the image plane onto the corresponding point in the laser plane, we are able to reconstruct the 2-D curve in the laser plane. Then moving the object step by step provides a dense map of the surface of the object.

A. Calibration Procedure

The calibration of our range finding system consists of estimating, for each camera, the geometric transformation that back-projects any point of image plane of the camera into the laser plane.

We have designed a physical calibration gauge consisting of

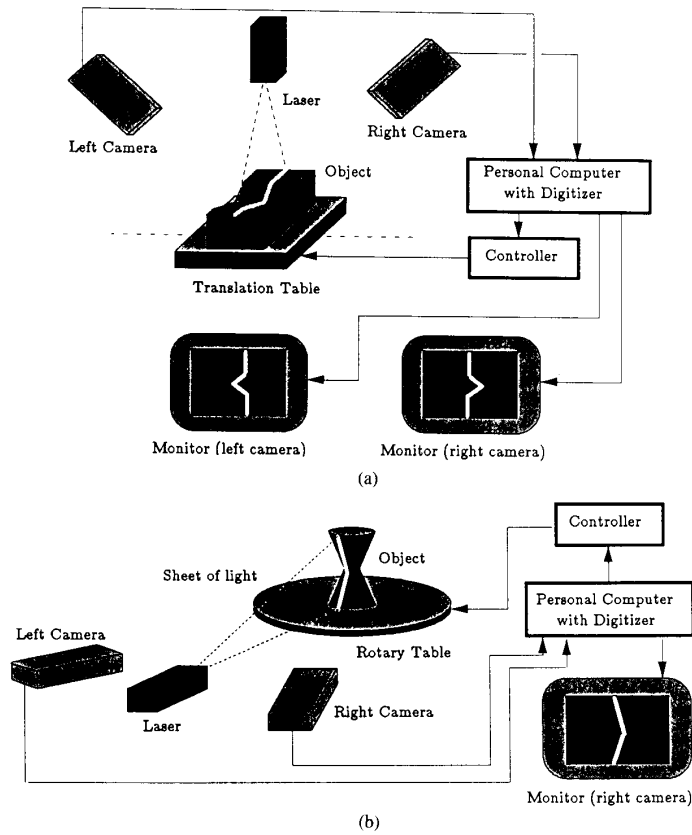


Fig. 1. Range-finding system configuration using (a) the linear table and (b) the rotary table.

horizontal plate and a vertical plate that, when fixed on the linear table ensures that its axis of translation is perpendicular to the vertical plate or that, when fixed on the rotary table ensures that its axis of rotation lies into the vertical plate (which we will call the gauge plane). Then, according to the size of the object to measure, a black and white pattern consisting of a white rectangle enclosed in a black rectangle is affixed on the gauge plane. Fig. 2(a) shows the calibration gauge placed upon the linear table, and Fig. 2(b) the calibration gauge placed upon the rotary table.

The first step of the calibration procedure requires aligning the laser plane with the gauge plane. Then the camera to calibrate is positioned so that the entire black and white pattern can be seen in the image plane [see Fig. 2(c)]. The second step of the calibration procedure estimates the geometric transformation from the image plane to the gauge plane (laser plane).

1) *Geometric Transformation Estimation:* Using homogeneous coordinates, the general transformation from a 3-D world to a 2-D world is given by a 3×4 matrix. In our case, the plane-to-plane transformation yields a 3×3 matrix. Thus, the transformation M_{cl} from the image plane coordinate system (O_c, X_c, Y_c) to the laser plane coordinate system (O_l, Y_l, Z_l) (see Fig. 3) is given by the following equations:

$$\begin{aligned}
 U &= M_{11}X_c + M_{12}Y_c + M_{13} \\
 V &= M_{21}X_c + M_{22}Y_c + M_{23} \\
 W &= M_{31}X_c + M_{32}Y_c + M_{33}
 \end{aligned}$$

and

$$\begin{aligned}
 Y_l &= U/W \\
 Z_l &= V/W.
 \end{aligned}$$

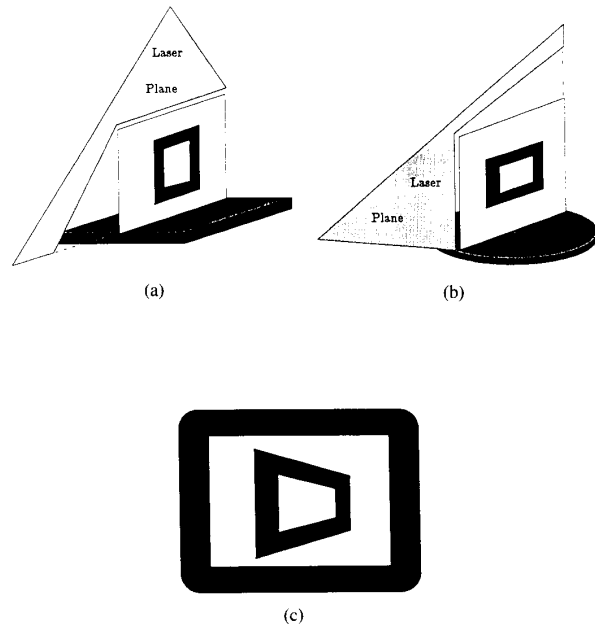


Fig. 2. Calibration procedure using (a) the linear table and (b) the rotary table. (c) Image of the calibration pattern.

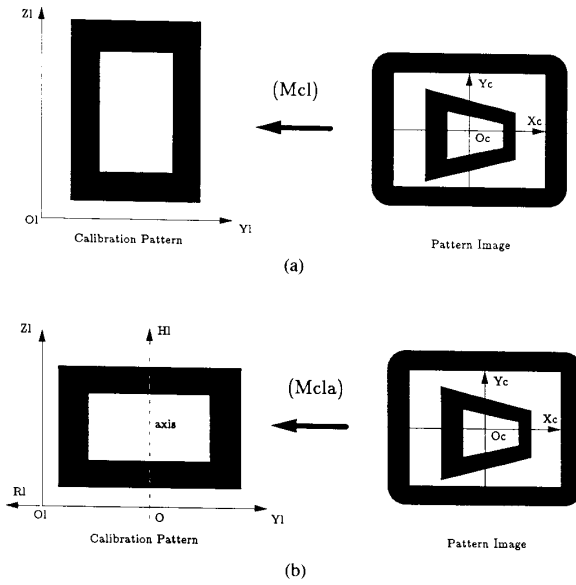


Fig. 3. Geometric transformations using (a) the linear table and (b) the rotary table.

Rewriting $U - Y_l W = 0$, $V - Z_l W = 0$, and setting M_{33} to 1 yields [1]

$$\begin{aligned} Y_l &= M_{11} X_c + M_{12} Y_c + M_{13} - Y_l M_{31} X_c - Y_l M_{32} Y_c \\ Z_l &= M_{21} X_c + M_{22} Y_c + M_{23} - Z_l M_{31} X_c - Z_l M_{32} Y_c. \end{aligned}$$

If more than four pairs of associated points $\{(X_c, Y_c), (Y_l, Z_l)\}$ are used, the eight parameters of the matrix M_{cl} can be estimated using a standard least square method [1]. In our case, we choose the eight corners of the black and white pattern attached to the gauge and their projections on the image plane as a set of points to perform this estimation using the pseudo-inverse method.

The corners of the pattern are given by their coordinates (Y_l, Z_l) in the gauge plane. The corresponding points in the image plane are detected by first extracting the lines corresponding to the four horizontal edges and four vertical edges of the pattern. This extraction is performed as follows:

At each point, the gradient is computed in a 3×3 window. From the direction of the gradient and the coordinates of the point, we compute the equation of the straight line passing through that point perpendicularly to the gradient direction. If there already exists a nonempty set of points approximately belonging to that line, the point is added to that set. Otherwise, a new set is created. This clustering is performed for significant values of the gradient only. Then the eight largest clusters are considered and each of them is fitted by a straight line using a standard least square method. The directions of the lines allow us to classify them as "horizontal" or "vertical." Finally, intersecting the "horizontal" lines with the "vertical" lines yields the eight corners (X_c, Y_c) .

Once the matrix M_{cl} has been computed, we can calculate the inverse matrix $M_{lc} = M_{cl}^{-1}$ in order to back-project the eight corners into the image plane and thus measure the estimation error. We have found that this method gives much better results (sub pixel accuracy) and is much faster than that which we first obtained using the Hough transform [1].

2) *Rotary Table:* When measuring objects using the rotary table, one would like to use cylindrical coordinates. In this case, one more step in the calibration procedure is required to compute the final matrix $M_{cla} = M_{axis} \cdot M_{cl}$, where M_{axis} represents the transformation from the coordinate system (O_l, Y_l, Z_l) to the coordinate system (O, R_l, H_l) [see Fig. 3(b)]. This problem is to find the axis of rotation of the rotary table in the coordinate system (O_l, Y_l, Z_l) ,

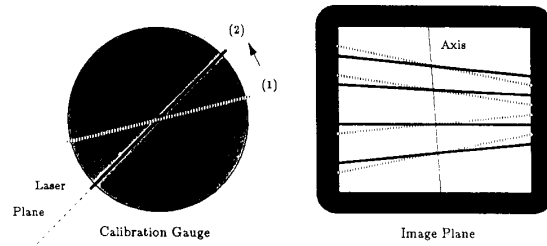


Fig. 4. Finding the axis of rotation.

that is, the points on the gauge plane that are invariant under the rotation of the gauge. We use the fact that any line in the gauge plane with the plane perpendicular to the axis of rotation passing through the camera axis) projected in the image plane yields a different line when rotating the gauge. The intersection of these corresponding lines belongs to the projection of the axis of rotation (see Fig. 4).

If we now consider the image of the black and white pattern, we can determine the projection of the axis of rotation by intersecting the corresponding "horizontal" lines resulting from a rotation of the gauge. Two points are enough, but performing a least square on the four points is better. Then, using M_{cl} , we can compute the axis of rotation in the laser plane coordinate system (O_l, Y_l, Z_l) and thus determine M_{axis} , which consists of a rotation followed by a translation and a symmetry with respect to OH_l .

The final matrix M_{cla} allows us to compute the distance R_l from the axis and the height H_l of the point in the laser plane corresponding to a point (X_c, Y_c) of the camera plane:

$$U = M_{11} X_c + M_{12} Y_c + M_{13}$$

$$V = M_{21} X_c + M_{22} Y_c + M_{23}$$

$$W = M_{31} X_c + M_{32} Y_c + 1$$

and

$$R_l = U / W$$

$$H_l = V / W.$$

Once one camera has been calibrated, the calibration of the second camera is performed exactly the same way. The only thing to do is to rotate the calibration gauge by 180° (the design of the gauge is such that the gauge plane still lies into the laser plane). The coordinate system in the laser plane is kept the same as for the calibration of the first camera.

3) *Comments:* As opposed to other similar existing systems [8], [11], it has been shown that our calibration procedure does not require any knowledge of the camera parameters and the relative position of the camera with the laser plane. Indeed, the only constraints are that we must align the laser plane with the gauge plane and make sure that the entire calibration pattern is in the field of view of the camera to calibrate. The calibration errors, which remain smaller than one pixel, show that our first-order approximation of the world-to-camera geometric transformation is legitimate. This fast and accurate calibration procedure is performed on the personal computer, the code is written in C, and the total calibration takes approximately 3 mn for each camera.

A picture of our system at the calibration level (using rotary table and a single camera) is shown in Fig. 5. The laser is located at the top left corner, the camera at the bottom, and the rotary table with the calibration gauge on the right of the picture.

B. Range and Intensity Data Acquisition

The measurement of a given object is performed as follows: for each camera and for every position s of the table, whether it is the linear or the rotary table, the projection of the 2-D curve intersecting the plane of light and the surface of the object (see Fig. 6) is

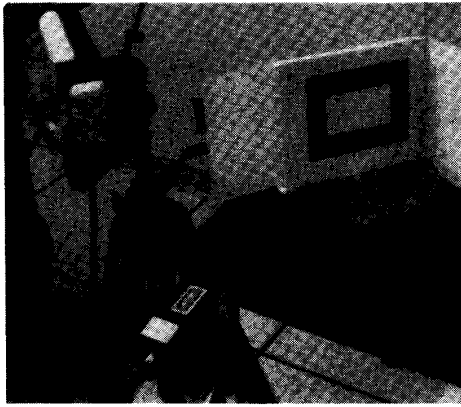


Fig. 5. Our system at the calibration level.

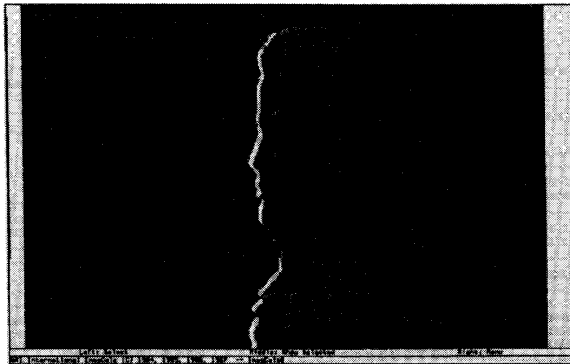


Fig. 6. Data acquisition.

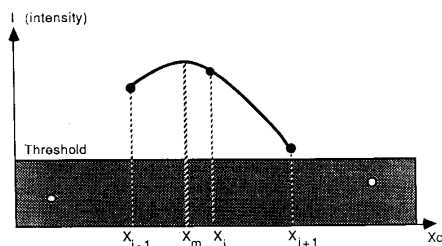


Fig. 7. Maximum detection with subpixel accuracy.

detected by scanning the image horizontally, looking for the maximum of intensity $I(X_c)$ along each row Y_c . These maxima are validated only when they are above a given threshold in order not to extract shiny areas of the object as part of the laser trace (notice that the best data acquisition is performed in a dark room or using a filter in the band of the laser). When a maximum has been detected along a given row Y_c , the maximum detection along the next row is performed only around the horizontal address X_c of this maximum.

As the precision of the position X_c of each maximum is limited by the camera resolution, we use the following interpolation method (see Fig. 7) to obtain subpixel accuracy, thanks to the width of the laser trace in the image, which is generally greater than five pixels. For each row Y_c , we consider the set of points consisting of the maximum $(X_i, I(X_i))$, its left neighbor $(X_{i-1}, I(X_{i-1}))$, and its right neighbor $(X_{i+1}, I(X_{i+1}))$. We fit a second-order polynomial to this set of points, from which we detect the maximum point $(X_m, I(X_m))$. As the solution X_m is given by a first-degree equation (by setting the derivative of the second-order polynomial equal to zero), this method does not add much computing time compared to simple maximum detection [7].

Using the calibration matrix corresponding to the active camera, we compute for each detected maximum (X_m, Y_c) the coordinates of the back-projected point in the laser plane, that is, (Y_l, Z_l) if using the linear table or (R_l, H_l) if using the rotary table. Furthermore, the interpolated intensity $I(X_m, Y_c)$ is kept as it directly measures the reflectance property of the object surface at this point in the wavelength of the laser light. The output of our system, after a complete displacement of the table, thus consists of three images for each camera, that is, $Y_l(u, v)$, $Z_l(u, v)$, and $I(u, v)$ if the linear table is used, or $R_l(u, v)$, $H_l(u, v)$, and $I(u, v)$ if the rotary table is used, where u and v , respectively, represent the row index Y_c in the image plane and the displacement s of the table.

C. Performance

The accuracy of our measurements is in the order of 0.25 mm for an object placed at approximately 0.5 m from the cameras, which is excellent for such a low-cost system. This estimation was performed by acquiring the range data of a perfectly planar object and computing the average error that resulted from fitting a plane to those data. Many results show later in this work illustrate the quality of these range measurements. The data acquisition takes about 4 s for each position of the linear or rotary table, which leads to approximately 15 mm for a typical scan (200 steps). But high speed is not the priority for this system, it was designed to provide good-quality range images at a low cost. Nevertheless, given the simplicity of the peak extraction and the small number of arithmetic operations required for the computation of the depth, special hardware could be designed that would speed up the data acquisition significantly. Finally, our simple peak extraction may lead to some errors whenever there are range discontinuities or multiple reflections of the laser beam on the surface the object to be measured, but this is the drawback of all plane-of-light methods. Experience has shown that these errors do not occur frequently, as will be seen in the results presented in the remainder of this paper.

III. DATA INTEGRATION

As we have seen in the previous section, our range finding system delivers two range images for each camera used, that is $Y_l(u, v)$ and $Z_l(u, v)$ if using the linear table, $R_l(u, v)$ and $H_l(u, v)$ if the rotary table is used. Although it is possible to directly process these data, it is very interesting to combine those images into a format more suitable for standard image processing/analysis techniques. When using the linear table, it is natural to expect a single range image $Z(X, Y)$ (cartesian coordinates) and with the rotary table, a single range image $R(\theta, H)$ (cylindrical coordinates), eventually combining the data obtained from the two cameras and thus limiting the occlusion problem. In the case of the rotary table, one would like also to arbitrarily set a cartesian coordinate system, and generate a corresponding cartesian image from the cylindrical image.

A. Single Camera

1) *Linear Table*: From two images $Y(u, v)$ and $Z(u, v)$, where u represents the row index in the camera image plane and v the displacement X along the linear table axis, we want to build the image $Z(X, Y)$. As the index v corresponds to the displacement X of the linear table along its axis, the problem is simply to combine for each value of X the 1-D discrete functions $Y(u)$ and $Z(u)$ into $Z(Y)$.

Given the extremal values Y_{\min} and Y_{\max} of the image $Y(u, v)$, we sample the interval $[Y_{\min}, Y_{\max}]$ at the same rate used for the displacement X of the linear table (in order to obtain a square grid). Then, for each sampled value Y (see Fig. 8), we compute the corresponding value(s) of Z by considering the continuous functions $Y_c(u)$ and $Z_c(u)$ obtained by linearly interpolating the values of the discrete functions $Y(u)$ and $Z(u)$. In the case where we find more than one value of Z corresponding to a given Y , we simply keep the highest value of Z .

2) *Rotary Table*: The same method is applied to generate the

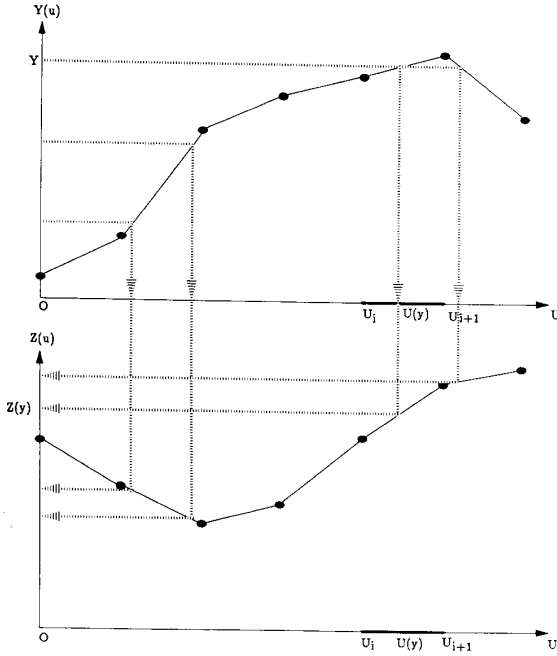


Fig. 8. Combining two 1-D discrete functions.

cylindrical image $R(\theta, H)$ from the two range images $R(u, v)$ and $H(u, v)$. In this case, the index v corresponds to the angle of rotation θ of the table around its axis. The problem is then simply to combine for each value of θ the 1-D discrete functions $R(u)$ and $H(u)$ into $R(H)$.

Given the extremal values H_{\min} and H_{\max} of the image $H(u, v)$, we sample the interval $[H_{\min}, H_{\max}]$ at an arbitrary rate, depending on the resolution wanted. Then, for each sampled value H , we compute the corresponding value(s) of R by considering the continuous functions $H_c(u)$ and $R_c(u)$ obtained by linearly interpolating the values of the discrete functions $H(u)$ and $R(u)$.

3) *From Cylindrical Image to Cartesian Image:* Although a cylindrical representation of the surface of an object is very useful, it is sometimes desirable to use Cartesian coordinates, for instance, to be able to use standard range image analysis techniques. Thus, given a cylindrical range image $R(u, v)$, one must choose a Cartesian coordinate system in which the three range images $X(u, v)$, $Y(u, v)$, and $Z(u, v)$ are to be computed. Finally, these range images must be combined into the Cartesian range image $Z(X, Y)$.

Given the extremal values X_{\min} and X_{\max} of the image $X(u, v)$, and the extremal values Y_{\min} and Y_{\max} of the image $Y(u, v)$, we sample the intervals $[X_{\min}, X_{\max}]$ and $[Y_{\min}, Y_{\max}]$ at the same rate (in order to obtain a square grid). Then, for each pair of sampled values X and Y (see Fig. 9), we compute the corresponding value(s) of Z by considering the continuous functions $X_c(u, v)$, $Y_c(u, v)$, $Y_c(u, v)$, and $Z_c(u, v)$ obtained by bilinearly interpolating the values of the discrete functions $X(u, v)$, $Y(u, v)$, and $Z(u, v)$. In the case where we find more than one value of Z corresponding to a given pair (X, Y) , we simply keep the highest value of Z .

B. Two Cameras

The integration of the data obtained from different sensors is a difficult task; we propose to conclude this section by showing how we address the problem in the case of our range finding system. Two subproblems can be found: the first one is to register the data obtained from the two cameras, and the second is to merge those data into a single range image.

1) *Data Registration:* Let us suppose that we use the linear

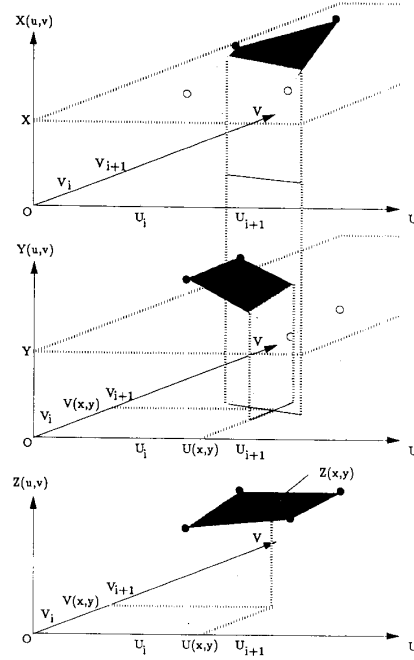


Fig. 9. Combining three 2-D discrete functions.

table, and that with the left camera we obtained the range images $Y_{\text{left}}(u, v)$ and $Z_{\text{left}}(u, v)$, and with the right camera, the range images $Y_{\text{right}}(u, v)$ and $Z_{\text{right}}(u, v)$. As the same laser plane coordinate system is used when calibrating the left and right cameras, the idea is to simply combine $Y_{\text{left}}(u, v)$ and $Z_{\text{left}}(u, v)$ into the Cartesian range image $Z_{\text{left}}(X, Y)$ and to combine $Y_{\text{right}}(u, v)$ and $Z_{\text{right}}(u, v)$ into $Z_{\text{right}}(X, Y)$. The same procedure is used when using the rotary table, that is, the range images $R_{\text{left}}(u, v)$ and $H_{\text{left}}(u, v)$ into the cylindrical range image $R_{\text{left}}(\theta, H)$ and to combine $R_{\text{right}}(u, v)$ and $H_{\text{right}}(u, v)$ into $R_{\text{right}}(\theta, H)$.

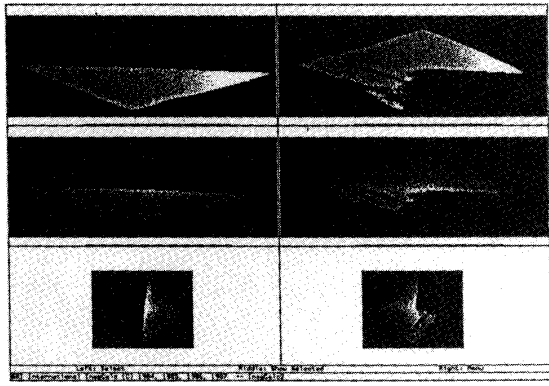
2) *Data Merging:* The final step is to merge the two range images $Z_{\text{left}}(X, Y)$ and $Z_{\text{right}}(X, Y)$ [or $R_{\text{left}}(\theta, H)$ and $R_{\text{right}}(\theta, H)$] into a single range image $Z(X, Y)$ [or $R(\theta, H)$]. The basic idea is to consider the left image (for example) and to fill the holes (occlusions) at the pixel level by picking the range value into the right image when the value is available. But as at a given point (u, v) where data are available in both images, we noticed that there is always a slight difference in the range caused by calibration errors or by the fact that, at the acquisition level, the laser peak may not correspond to the same point on the object surface, and this filling procedure cannot be done directly.

Instead, we first compute the difference image $D(X, Y) = Z_{\text{right}}(X, Y) - Z_{\text{left}}(X, Y)$ at these points where data are available in both images. From this difference image, we compute an error function $E(X, Y)$ by globally fitting a plane using the available points in $D(X, Y)$. Only then, at any point (X, Y) where there is a hole in the left image, is its range value set to $Z_{\text{right}}(X, Y) - E(X, Y)$.

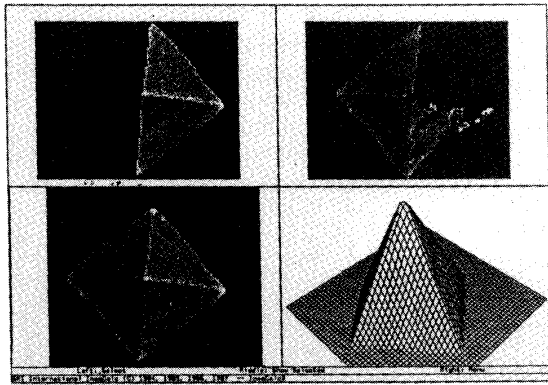
C. Example

To illustrate the ideas previously introduced, we show in Fig. 10 the intermediate results obtained at each step using range data acquired from a simple polyhedral object, a pyramid. This object has been measured using the linear table and two cameras. The results for the left and right camera are displayed in the left and right column, respectively.

Fig. 10(a) shows the first step, which, for each camera, combines



(a)



(b)

Fig. 10. Intermediate results.

$Y(u, v)$ (first row) with $Z(u, v)$ (second row). The resulting Cartesian range images $Z(X, Y)$ are shown on the last row. Notice for each camera the occluded areas where no data are available.

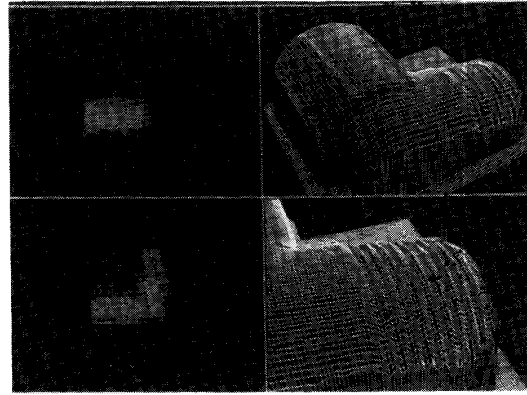
Fig. 10(b) shows the second step, which merges both Cartesian range images $Z_{\text{left}}(X, Y)$ and $Z_{\text{right}}(X, Y)$ (displayed on the top row) into a single Cartesian range image $Z(Z, Y)$ (displayed at the bottom left corner). A 3-D view of the latter image is shown at the bottom right corner. Notice that most occlusions have disappeared and that the range information from the two views is smoothly integrated.

IV. DATA ACQUISITION FROM COMPLEX OBJECTS

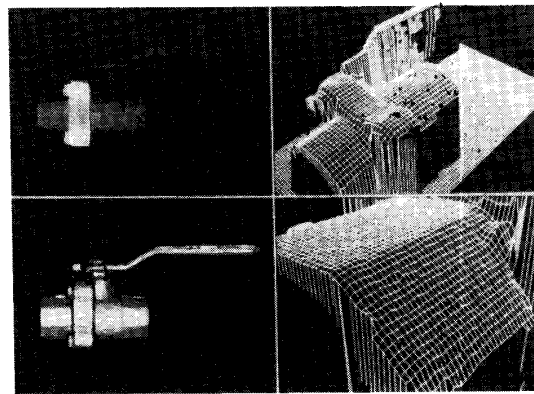
To illustrate the versatility of our range finding system, we show in this section results obtained for complex objects measured using the linear table or the rotary table with one or two cameras. It is important to point out that *no* smoothing or any other processing was applied to the range images shown. As explained in the previous section, the final format of the range images is $Z(X, Y)$, the resolution depending on the step size chosen for the linear or rotary table at the time of acquisition.

The first objects we consider are mechanical parts (see Fig. 11) for which we used the linear table and two cameras. For each object, we show the resulting Cartesian range image in the upper left corner, the corresponding shaded image in the lower left corner, and two 3-D plots at different resolutions on the right column. As one can notice, the detailed 3-D plot (for which full resolution is used) shows how well the surface of the object is accurately measured with almost no noise added. We have successfully used these range images for the description of the corresponding objects using their surface properties [5].

The results of the acquisition of range data for a Mozart bust, for



(a)



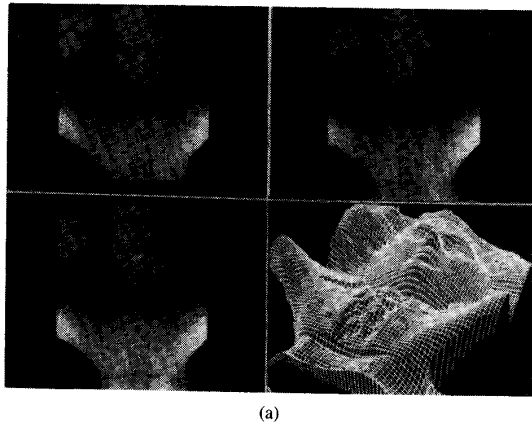
(b)

Fig. 11. Mechanical parts.

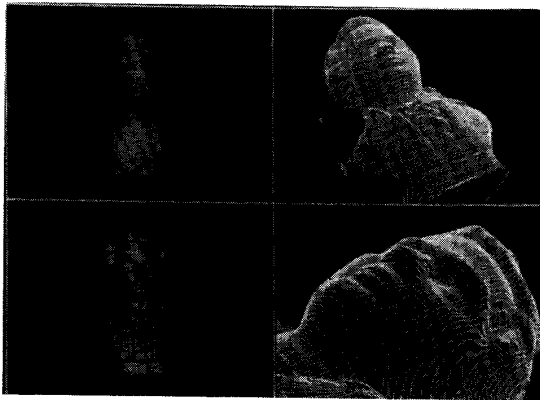
which we used the rotary table and two cameras, are shown in Fig. 12. Fig. 12(a) first shows how the left and right cylindrical range images (upper row) are merged into a global cylindrical range image (lower left corner) for which we show a 3-D plot in the lower right corner. Almost all occlusion spots have disappeared, the merging of the data having been done successfully. The next picture [Fig. 12(b)] shows, after having chosen a Cartesian coordinate system, the Cartesian range image obtained. Again, the Cartesian range image is displayed in the upper left corner, and the corresponding shaded image in the lower left corner, and two different 3-D plots on the right column (none of them uses full resolution because of the image size, which explains why the surface appears smoother than for the mechanical parts).

All that the previous objects have in common is that they are all white or have been painted (matte) white. But this is not necessary. As a first example, Fig. 13 shows the Cartesian range image (upper left corner) obtained from a Renault part whose surface is highly textured, and whose reflectance properties vary. For this object, we used the linear table with a single camera. The corresponding shaded image is displayed in the upper right corner, while a 3-D plot is drawn in the lower right corner. Finally we show in the lower left corner the Cartesian intensity image (in registration with the Cartesian range image) obtained from the left camera by measuring the intensity of the laser peak. These results are very interesting as they can be used as a ground truth for algorithms such as stereo or shape from shading.

Finally, by still using the linear table with a single camera, we show the results obtained for a very complex object such as a PC board (Fig. 14). The Cartesian range image is shown in the upper left corner, the registered intensity image in the lower left corner.



(a)



(b)

Fig. 12. Mozart bust.

We concentrated on a small area of the board (upper right corner) to display a 3-D plot at full resolution of the Cartesian range image in this area. The latter shows that, globally, despite the presence of multiple reflections of the laser beam and many range discontinuities, the range image of the board has been acquired successfully.

V. CONCLUSION

We have designed and built a range finding system which, we think, besides its low cost, has several advantages over similar existing systems. It is designed to use two cameras so that the well-known occlusion problem can be significantly reduced. The calibration of each camera is very simple and accurate (subpixel accuracy) and is performed only once as the laser or the camera do not move. Although our range acquisition is simple (and thus could be easily implemented in hardware), our interpolation method for the laser peak extraction allows us to obtain very accurate results (typically 0.25 mm for an object placed at 0.5 m from the cameras). By taking the interpolated intensity of the laser light at the peak location, we also provide intensity images in registration with the range images. Finally, the choice between a linear or a rotary table permits the acquisition of range data for various objects and permits a choice between two different representations, that is Cartesian or cylindrical coordinates. Already two different applications, that is 3-D object recognition [5] and robot hand-eye coordination [10], make use of our range finding system. A complete description, including the code to perform all the operations described in this work, is available for all interested parties.

ACKNOWLEDGMENT

The authors would like to express their sincere gratitude to P. J. Lin for his help with the implementation phase of this range finding system.

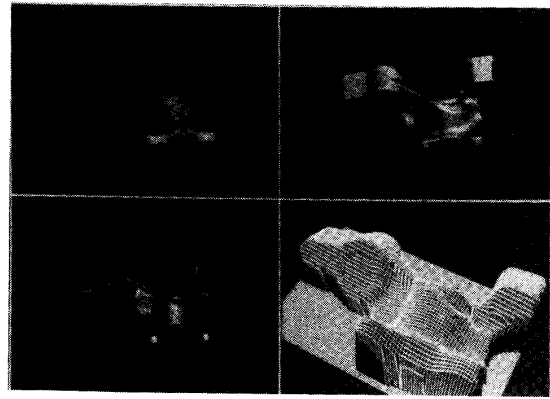


Fig. 13. Renault part.

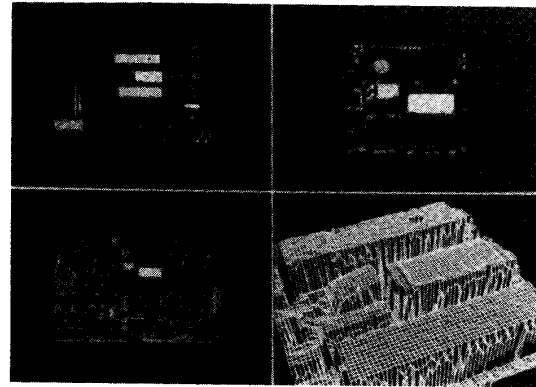


Fig. 14. PC board.

REFERENCES

- [1] D. H. Ballard and C. M. Brown, *Computer Vision*. Englewood Cliffs, NJ: Prentice-Hall, 1982.
- [2] P. J. Besl, "Range imaging systems," General Motors Res. Labs., Warren, MI, Tech. Rep., 1988.
- [3] P. J. Besl and R. C. Jain, "Three-dimensional object recognition," *ACM Computing Surveys*, vol. 17, no. 1, pp. 75-145, 1985.
- [4] D. Dementhon, T. Siddalingaiah, and L. S. Davis, "Production of dense range images with the CVL light-stripe/range scanner," Center for Automation Res., Univ. of Maryland, Tech. Rep., 1987.
- [5] T. J. Fan, "Describing and recognizing 3-D objects using surface properties," Ph.D. dissertation 237, Institute for Robotics and Intelligent Systems, School of Engineering, Univ. of Southern California, Los Angeles, CA, Aug. 1988.
- [6] R. A. Jarvis, "A perspective on range finding techniques for computer vision," *IEEE Trans. Pattern Anal. Machine Intell.*, vol. PAMI-5, no. 2, pp. 122-139, Mar. 1983.
- [7] J. L. Jezouin, P. Saint-Marc, and G. Medioni, "Building an accurate range finder with off the shelf components," in *Proc. IEEE Computer Vision and Pattern Recognition* (Ann Arbor, MI), 1988, pp. 195-200.
- [8] S. Lelandais, "Réalisation et première exploitation d'un système de numérisation de formes tridimensionnelles," ENST, Tech. Rep. 84E004, Apr. 1984.
- [9] S. Parthasarathy, J. Birk, and J. Dessimoz, "Laser range-finder for robot control and inspection," in *Proc. SPIE Robot Vision*, May 1982, pp. 2-11.
- [10] K. Rao, G. Medioni, H. Liu, and G. Bekey, "Robot hand-eye coordination: Shape description and grasping," in *Proc. IEEE Int. Conf. Robotics Automat.* (Philadelphia, PA), Apr. 1988, pp. 407-411.
- [11] Y. Sato, H. Kitagawa, and H. Fujita, "Shape measurement of curved objects using multiple slit-ray projections," *IEEE Trans. Pattern Anal. Machine Intell.*, vol. PAMI-4, no. 6, pp. 641-646, Nov. 1982.
- [12] *100A White Scanner User's Manual*, Technical Arts Corp.